



# Antiproliferative activity and apoptosis induction, of organo-antimony(III)–copper(I) conjugates, against human breast cancer cells

C. N. Banti<sup>1</sup> · V. Tsiatouras<sup>1</sup> · K. Karanicolas<sup>1</sup> · N. Panagiotou<sup>2</sup> · A. J. Tasiopoulos<sup>2</sup> · N. Kourkoumelis<sup>3</sup> · S. K. Hadjikakou<sup>1</sup>

Received: 25 September 2019 / Accepted: 2 November 2019  
© Springer Nature Switzerland AG 2019

## Abstract

Three known organo-antimony(III)–copper(I), mixed-metal small bioactive molecules (SBAMs) of formula [Cu(tpSb)<sub>3</sub>Cl] (**1**), [Cu<sub>2</sub>(tpSb)<sub>4</sub>Br<sub>2</sub>] (**2**) and [Cu<sub>2</sub>(tpSb)<sub>4</sub>I<sub>2</sub>] (**3**) (tpSb = triphenylstibine) were used for the clarification of their antiproliferative activity against human breast cancer cells: MCF-7 (hormone-dependent cells) and MDA-MB-231 (hormone-independent cells). The *in vitro* toxicity of **1–3** was studied against normal human foetal lung fibroblast cells (MRC-5). The genotoxicity of **1–3** was determined by the presence of micronucleus. The type of the cell death caused by **1–3** was determined using cell cycle arrest. The molecular mechanism of action of **1–3** was defined by their binding affinity towards CT-DNA (calf thymus DNA) using UV spectroscopy and viscosity measurements. Docking studies depict the interactions between **1–3** and DNA. Computations were also employed in order to rationalize the activity of these compounds. This is based on the contribution of metal aromaticity in the case of compounds **2** and **3** where the short Cu...Cu distance (2.7724(6) (**2**) and 2.7251(11) (**3**) Å, respectively) suggests *d*<sup>10</sup>–*d*<sup>10</sup> interaction between metal centres.

---

**Electronic supplementary material** The online version of this article (<https://doi.org/10.1007/s11030-019-10014-z>) contains supplementary material, which is available to authorized users.

---

- ✉ C. N. Banti  
cbanti@uoi.gr
- ✉ N. Kourkoumelis  
nkourkou@uoi.gr
- ✉ S. K. Hadjikakou  
shadjika@uoi.gr

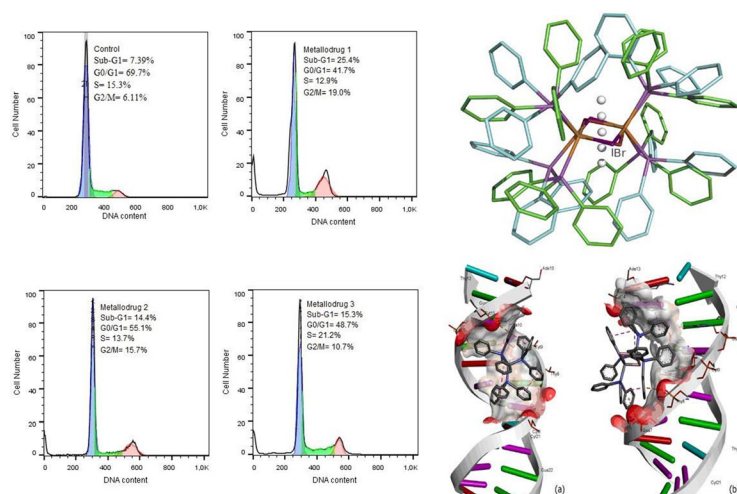
<sup>1</sup> Section of Inorganic and Analytical Chemistry, Department of Chemistry, University of Ioannina, 45110 Ioannina, Greece

<sup>2</sup> Department of Chemistry, University of Cyprus, 1678 Nicosia, Cyprus

<sup>3</sup> Medical Physics Laboratory, Medical School, University of Ioannina, Ioannina, Greece

## Graphic abstract

The known small bioactive molecules of formula  $[\text{Cu}(\text{tpSb})_3\text{Cl}]$  (**1**),  $[\text{Cu}_2(\text{tpSb})_4\text{Br}_2]$  (**2**) and  $[\text{Cu}_2(\text{tpSb})_4\text{I}_2]$  (**3**) (tpSb = triphenylstibine) were used for the clarification of their antiproliferative activity against human breast cancer cells: MCF-7 (hormone-dependent (HD) cells) and MDA-MB-231 (hormone-independent (HI) cells).



**Keywords** Metal biology · Metallotherapeutics · Copper(I)–antimony(III) complexes · Cytotoxic activity · Breast cancer

## Introduction

The most frequent malignancy in women worldwide is breast cancer [1]. The molecular features of breast cancer include activation of human epidermal growth factor receptor 2, activation of hormone receptors (oestrogen receptor and progesterone receptor) and/or mutations in the tumour suppressor genes [1, 2]. Most breast cancers are oestrogen receptors (ER) positive, which have a relatively good prognosis [3]. However, limited targeted therapies are available for the most aggressive ER-negative breast cancers, “triple negative” breast cancers (TNBC) [3]. Human breast cancer MCF-7 and MDA-MB-231 cells are both breast carcinoma cells, which have, however, many phenotypic/genotypic differences: MCF7 are hormone-dependent (both positive to oestrogen (ER) and progesterone (PR) receptors) [4], while MDA-MB-231 are triple negative that lack oestrogen and progesterone receptors and human epidermal growth factor receptor 2 (HER2) [5].

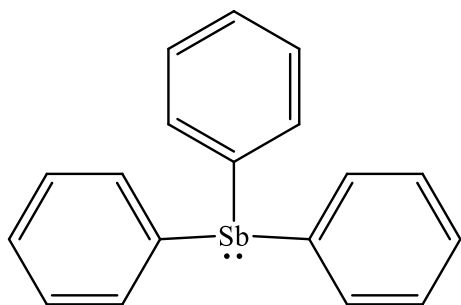
Copper(II) compounds, on the other hand, have been intensively studied; however, the corresponding ones of Cu(I) have been scarcely tested as antimicrobial, antiviral, antifungal and anticancer drugs due to their significant lower stability in water media [6]. Moreover, copper(I) complexes are expected to be less toxic to normal cells in contrast to tumour ones, due to the physiological properties of copper as endogenous metal [7]. Antimony(III) compounds exhibit

antiproliferative properties and have been tested in both normal and cancerous cells with promising results [8].

In the course of our studies in the development of novel metallodrugs [2, 9–17], the known organo-antimony(III)–copper(I) mixed-metal small bioactive molecules (SBAMs) of formula  $[\text{Cu}(\text{tpSb})_3\text{Cl}]$  (**1**),  $[\text{Cu}_2(\text{tpSb})_4\text{Br}_2]$  (**2**) and  $[\text{Cu}_2(\text{tpSb})_4\text{I}_2]$  (**3**) (tpSb = triphenylstibine, Scheme 1) were tested against MCF-7 (hormone-dependent (HD)) and MDA-MB231 (hormone-independent (HI)) cells. Their toxicity of **1–3** was evaluated against MRC-5. Further, their genotoxicity was determined by the presence of micronucleus. The type of the cell death caused by metallodrugs was determined using cell cycle arrest assay. The molecular mechanism of their action was evaluated towards CT-DNA (calf thymus DNA) using UV spectroscopy and viscosity measurements.

## Results and discussion

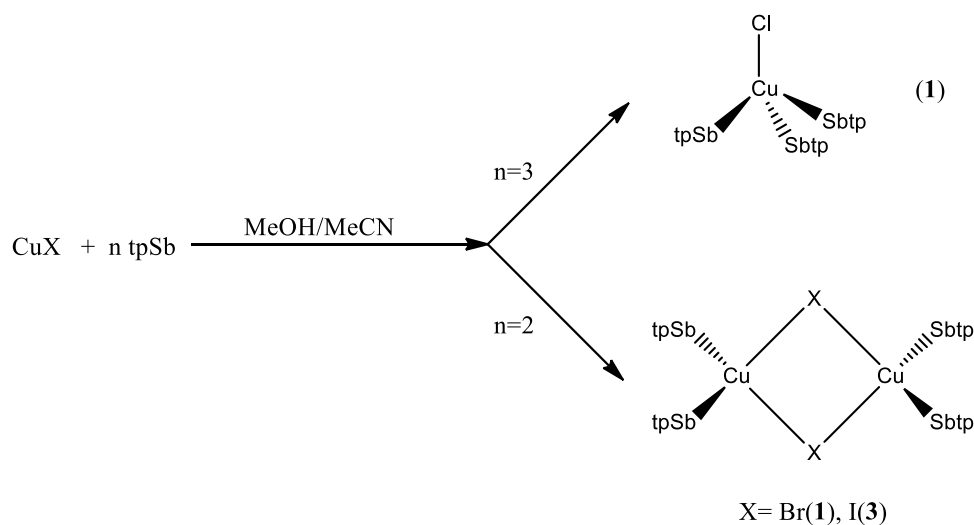
**General aspects** Although **1–3** are known, they were obtained here by an alternative method which is described briefly.  $\text{CuX}$  (Cl(**1**), Br(**2**) and I(**3**)) react with  $\text{Ph}_3\text{Sb}$  in 1:3 (**1**) and 1:2 (**2** and **3**) molar ratios in methanol/acetonitrile solution under reflux (Reaction 1). Pure **1–3** in crystalline form were obtained by slow evaporation of the methanol/acetonitrile solution which remains after the filtration of the



**Scheme 1** Molecular formula of tpSb

reaction solution. Air-stable crystals of **1–3** were analysed by X-ray diffraction crystallography.

$b = 15.5253(5)$ ,  $c = 21.8157(8)$  Å,  $\alpha = 77.178(3)$ ,  $\beta = 84.177(3)$ ,  $\gamma = 81.118(3)^\circ$ , on the other hand, varied from the corresponding one of **COWBOF**; space group P-1,  $a = 13.827(3)$ ,  $b = 14.279(3)$ ,  $c = 14.399(3)$  Å,  $\alpha = 84.43(2)$ ,  $\beta = 87.39(2)$ ,  $\gamma = 75.18(1)^\circ$ ,  $R = 0.00636$  [21] due to the solvent molecule which is co-crystallized in this case. Thus, although the molecular formula of **1** has been reported by Reichle, previously [22], its crystal structure is a polymorphic one to **COWBOF** reported by Rheingold et.al [21]. Therefore, the preparation and crystallization media used in case of **COWBOF** (hexane/dichloromethane), towards methanol/acetonitrile used in **1**, sets the crystallization system. This is why the crystal structure determination of **1** was



**Reaction 1.** Preparation routes of **1–3**

### Solid-state studies

*Crystal structure of  $[Cu(tpSb)_3Cl]$  (**1**),  $[Cu_2(tpSb)_4Br_2]$  (**2**) and  $[Cu_2(tpSb)_4I_2]$  (**3**)* The molecular and crystal structures of **2–3** are known. The unit cell of **2** is: space group P 21/c,  $a = 24.1564(8)$ ,  $b = 14.0156(4)$ ,  $c = 19.8556(7)$  Å,  $\beta = 110.116(4)^\circ$ , while the corresponding of the known **NUHQOW** is: P 21/c,  $a = 24.336(7)$ ,  $b = 14.214(4)$ ,  $c = 20.097(7)$  Å,  $\beta = 109.91(2)^\circ$  [18]. The unit cell of **3**: space group P 21/c,  $a = 24.4375(4)$ ,  $b = 13.9106(2)$ ,  $c = 20.2194(3)$  Å,  $\beta = 111.169(2)^\circ$ ; **NUHQUC**: P 21/c,  $a = 24.620(9)$ ,  $b = 14.090(4)$ ,  $c = 20.382(9)$  Å,  $\beta = 110.65(3)^\circ$  [18], **NUHQUC01**: space group P 21/a,  $a = 20.436(5)$ ,  $b = 14.125(3)$ ,  $c = 24.683(3)$  Å,  $\beta = 110.67(1)^\circ$  [19], **NUHQUC02**: space group P 21/c,  $a = 24.4463(6)$ ,  $b = 13.9088(3)$ ,  $c = 20.2168(5)$  Å,  $\beta = 111.241(3)^\circ$  [20]. The crystal structure of **1**; space group P-1,  $a = 14.1646(5)$ ,

refined and reported here again. Moreover, since no biological data are available for these compounds (**1–3**) up to now, their antiproliferative activities were evaluated.

Molecular diagrams of **1–3** are shown in Fig. 1.

*Vibrational spectroscopy* The vibration bands at  $3066\text{ cm}^{-1}$  in FT-IR spectra of **1–3** (Figures S1–S2) are attributed to the C-H bond of the aromatic ring of tpSb. The corresponding one for free ligand tpSb is observed at  $3062\text{ cm}^{-1}$ . The vibration band at  $448\text{ cm}^{-1}$  in the FT-IR spectrum of tpSb which is attributed to the  $\nu_{\text{sym}}(\text{C-Sb})$  is shifted at  $453$  (**1**),  $461$  (**2**) and  $461$  (**3**)  $\text{cm}^{-1}$ , suggesting coordination of the ligand in the metal centre [23].

### Solution studies

*Stability studies* The retention of the structures of **1–3** in solution was checked by  $^1\text{H-NMR}$  spectroscopy, in dms- $d_6$  solution (Figures S3–S5). No changes were observed

between the initial spectrum and the corresponding after 48 h.

**<sup>1</sup>H NMR studies** The multiple resonance signals at 7.39–7.30 ppm are due to the  $H_{\text{aromatic}}$  of free tpSb, which are shifted at 7.43–7.36 (1), 7.43–7.36 (2) and 7.42–7.36 (3) ppm, respectively, in the case of the spectra of 1–3 (Figure S6).

**Nucleus-Independent Chemical Shifts (NICS) studies** The cuprophilicity which is observed in 2 and 3 by unexpected short Cu...Cu distances (2.7724(6) (2) and 2.7251(11) (3) Å, respectively) prompts us to apply NICS [24] for the investigating these Cu–Cu bonding interactions by magnetic criteria. The electron density delocalization of the molecular orbitals involved in the Cu<sub>2</sub>Br<sub>2</sub> and Cu<sub>2</sub>I<sub>2</sub> cores can possibly provide increased stability to the overall molecular structures. Clusters with transition-metal can exhibit d-orbital aromaticity or δ-aromaticity due to δ bonding interactions. Yet, for d-orbital aromaticity to occur significant d–d bonding interactions are essential. The tendency of d orbitals to participate in chemical bonding depends strongly on the coordination environment due to their spatial arrangement [25]. In this work, the four-membered aromatic clusters are stabilized by two bridging Br or I atoms adjacent to Cu atoms exhibiting Cs symmetry but with the I analog organized in a wider area with increased Cu–I bond lengths. The distance d(Cu–I) is approximately 0.2 Å larger than the corresponding d(Cu–Br). NICS indices are the negative isotropic values of the absolute NMR shielding at distances ranging from 2.0 to +2.0 Å along the vertical C2 axis (Fig. 2, white spheres) of the clusters. NICS(0) values near –8 ppm, indicate aromaticity since, at the same level of theory, the corresponding value for benzene is –8.5 ppm, while NICS(0) values close to zero represent non-aromaticity. NICS(0) (i.e., at 0 Å) of the Br analog was calculated to –2.4 ppm, while for the I analog it was –6.6 ppm. NICS(1) values are lower by 4.2 ppm for complex 3 and practically zero at NICS(2). The results suggest the presence of induced diatropic ring current at the molecular plane of Cu<sub>2</sub>I<sub>2</sub> and not at Cu<sub>2</sub>Br<sub>2</sub>, confirming that metal aromaticity is strongly affected by the metal coordination and halogen type.

**Antiproliferative studies** The metallodrugs 1–3 were tested for their *in vitro* antiproliferative activity against human breast adenocarcinoma cell lines: MCF-7 (hormone-dependent cells), MDA-MB-231 (hormone-independent cells) and the non-cancerous cell line, MRC-5 (normal human foetal lung fibroblast cells), by the sulforhodamine B (SRB) assay [23] (Table 1). The cells were incubated for 48 h with the metallodrugs. The IC<sub>50</sub> values of 1–3 towards MCF-7 cells are 11.1 ± 0.4 (1), 9.2 ± 0.5 (2) and 18.4 ± 1.4 (3) μM, respectively, while against MDA-MB 231 cells are 7.3 ± 0.3 (1), 6.4 ± 0.2 (2) and 11.2 ± 1.1 (3) μM, respectively. Therefore, a selectivity of 1–3 towards the hormone-independent MBA-MB 231 cancer cells than

the hormone-dependent MCF-7 ones is observed. Moreover, the IC<sub>50</sub> of cisplatin, a commercial drug of clinical used, is 5.5 ± 0.4 μM, and against MDA-MB 231 cells, it is 26.7 ± 1.1 μM. Therefore, 1–3 show two- to fourfold higher activity against MBA-MB 231 cells than cisplatin.

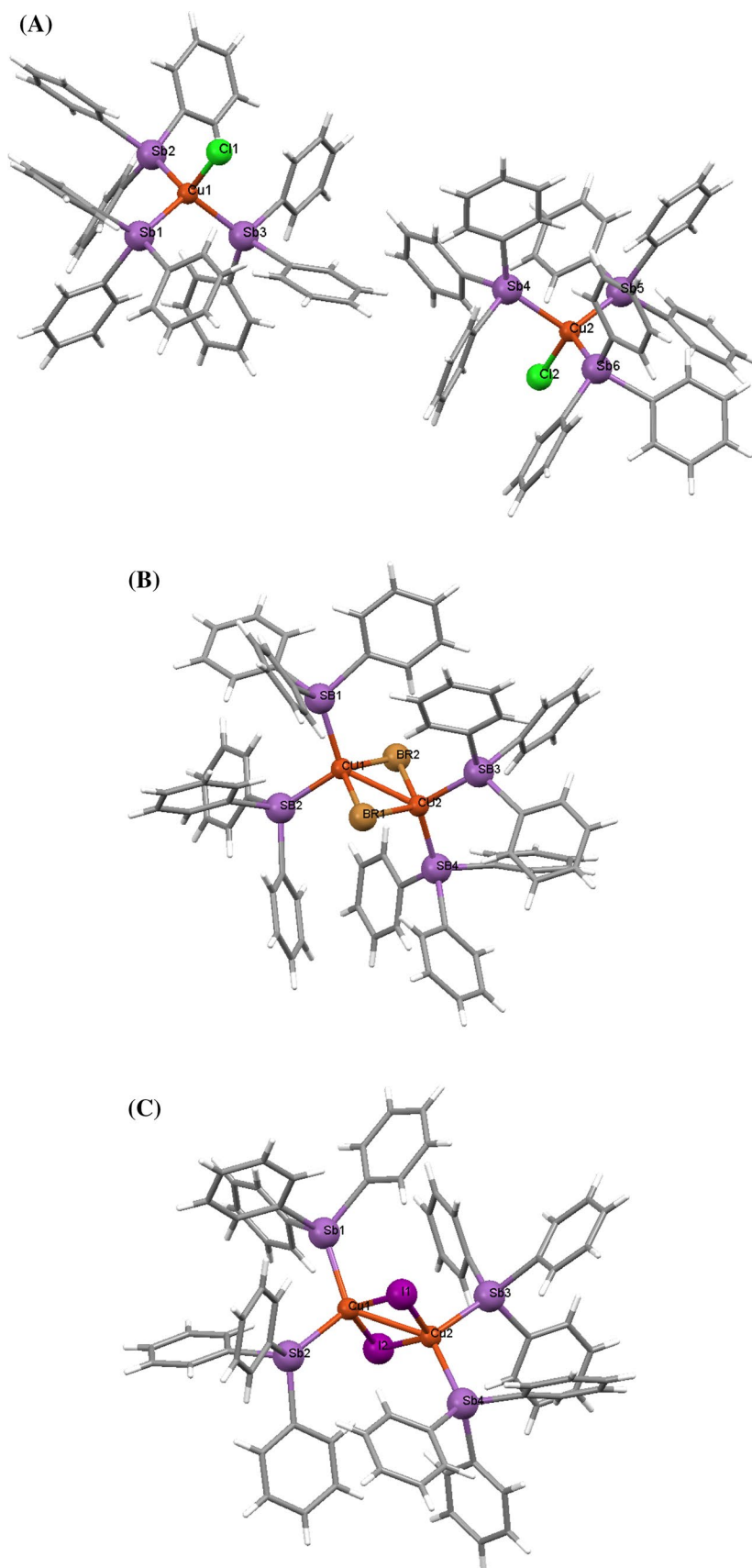
The homoleptic compounds 1–3, on the other hand, exhibit stronger activity than the corresponding heteroleptic ones of formulae [CuX(μ<sub>2</sub>-S)-tzdtH(tpSb)]<sub>2</sub> (X = Cl, Br and I; tzdtH = 2-mercapto-thiazolidine) (Table 1). This activity is four times higher against MDA-MB 231 and two times when MCF-7 cells are used [23]. Therefore, the substitution of one ligand in the coordination sphere of Cu(I) by a tzdtH ligand weakens their biological activity [23]. Thus, compounds 1–3 not only exhibit selectivity against the breast cancer cells without hormone receptors (MDA-MB 231), which is higher even than that of cisplatin as well, but also exhibit stronger activity than the corresponding one of the heteroleptic Cu(I) complexes of tpSb [23].

The *in vitro* toxicity of 1–3 was tested against the non-cancerous cell line, MRC-5 (normal human foetal lung fibroblast cells) (Table 1). The IC<sub>50</sub> values against MRC-5 cells are 9.9 ± 0.5 (1), 5.1 ± 0.1 (2) and 8.1 ± 0.2 (3) μM, respectively. The therapeutic potency index (TPI) which is defined as the IC<sub>50</sub> value against normal cells towards the IC<sub>50</sub> against cancerous ones is 1.4 (1), 0.8 (2) and 0.7 (3), respectively, in case of MDA-MB 231 and 0.9 (1), 0.6 (2) and 0.4 (3), respectively, against MCF-7 cells (Table 1) [9]. The corresponding TPI values of cisplatin against MDA-MB-231 and MCF-7 cells are 0.8 and 0.9, respectively. Therefore, the effectiveness of 1–3 is better than corresponding one of cisplatin.

The micronucleus (MN) assay was employed for the evaluation of the *in vitro* genotoxicity of 1–3. The MRC-5 cells were incubated for 48 h, with 1–3 at their IC<sub>50</sub> values, and the micronucleus frequencies were checked (Figure S7). The micronucleus frequency (%) in the case of the non-treated cells is 1.0 ± 0.2. This remains unchanged when MRC-5 cells were treated with 1–3, 1.0 ± 0.1 (1), 1.3 ± 0.4 (2) and 1.2 ± 0.2 (3) %, respectively. When MRC-5 cells are incubated with cisplatin, the MN frequency is 1.6% [9]. Therefore, 1–3 are causing less genetic damage against the normal MRC-5 than cisplatin.

**Cell cycle arrest** One of the main characteristics of apoptosis is the internucleosomal DNA fragmentation, which can be identified by the presence of sub-G<sub>1</sub> peak on DNA content histograms [26]. In order to evaluate the effect of the cell cycle arrest of MCF-7 cells, upon their treatment with 1–3 at IC<sub>50</sub> values, flow cytometric analysis was performed. The percentage of cells in various phases of the cell cycle was analysed and it is presented as the number of cells versus DNA content in different phases of cell cycle (sub-G<sub>1</sub>, G<sub>0</sub>/G<sub>1</sub>, S and G<sub>2</sub>/M) (Fig. 3).

**Fig. 1** Molecular diagrams together with the numbering scheme of **1** (A), **2** (B) and **3** (C) compounds. Selected bond distances (Å) are: **1\_MOLECULE-A**: Cu1-Cl1 = 2.2367(15), **1\_MOLECULE-B**: Cu2-Cl2 = 2.2699(15); **2**: Cu1-Br1 = 2.5079(7), Cu1-Br2 = 2.4703(6), Cu1-Br2 = 2.4507(6), Cu2-Br2 = 2.4989(7), Cu1-Cu2 = 2.7724(6); **3**: Cu1-I1 = 2.6502(9), Cu2-I1 = 2.6188(9), Cu1-I2 = 2.6338(7), Cu2-I2 = 2.6424(9)



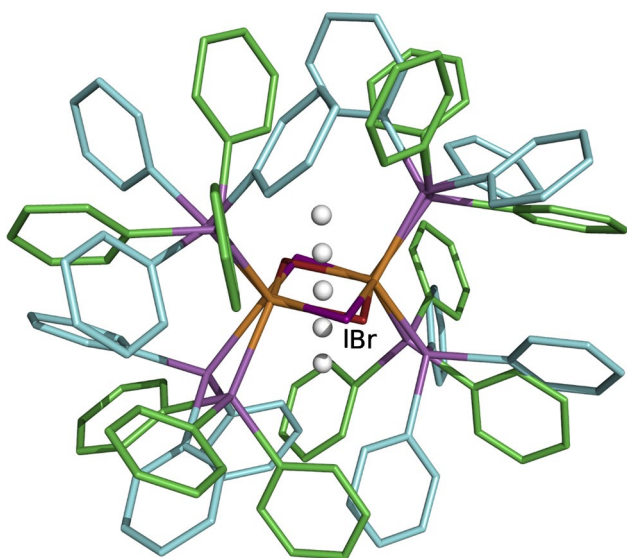


**Fig. 2** Superimposed structures with the  $\text{Cu}_2\text{Br}_2$  and  $\text{Cu}_2\text{I}_2$  cores and the vertical axis along which NICS values have been calculated by placing “ghost” atoms

The untreated cells are spread by 7.39% in sub- $G_1$  phase, 69.7% in  $G_0/G_1$ , 15.3% in S and 6.11% in  $G_2/M$  phases (Fig. 3). However, upon incubation of MCF-7 cells with the **1–3**, the percentage of the cells in the sub- $G_1$  phase is increased at 25.4% (**1**), 14.4% (**2**) and 15.3% (**3**), respectively, in respect of the untreated cells which are in sub- $G_1$  phase (7.39%), indicating the apoptotic type of the death of MCF-7 cells.

The percentage of cells in  $G_2/M$  phase is increasing in the metallodrugs **1–3** (19.0% (**1**), 15.7% (**2**) and 10.7% (**3**)), in contrast to 6.11% for the untreated cells. Metallodrugs **1–3** accumulate cancer cells at the  $G_2/M$  phase of their cycle by delaying or inhibiting cell cycle progression at the  $G_2/M$  phase [27]. The damaged cells stop DNA replication at  $G_2$

phase, presumably allowing cells to repair DNA lesions prior to mitosis [28]. The percentage of cells is also increasing in the S phase (21.2%) towards to the untreated cells (15.3%) in the case of **3**. Thus, **3** accumulates the cells in  $G_2/M$  and S phases simultaneously; as a result, it suppresses the cell proliferation by inhibiting DNA synthesis.

The cisplatin causes cell cycle arrest at S and  $G_2/M$  phases and the percentage of MCF-7 cells in sub- $G_1$  phase is increased, exhibiting an increasing number of apoptotic cells [9, 29]. Overall, these metallodrugs reduce the cell growth by induction of apoptotic type of cell death, in a similar manner to cisplatin.

**DNA binding studies** Metallodrugs bind either covalently or non-covalently to DNA. Non-covalent modes by which metal complexes bind to DNA include among others intercalation, groove binding, intercalation between the stacked base pairs of native DNA, etc [9]. However, the type of the particular specific molecular interactions of copper compounds with DNA is still not clearly established [30, 31]. In order to elucidate how copper compounds **1–3** interact with DNA, their binding studies were performed by UV absorption spectroscopy and viscosity.

(a) **UV absorption spectroscopy** In order to confirm the apoptotic mechanism of cells death which has been suggested by cell cycle arrest, the interaction of **1–3** interaction with CT-DNA was examined by UV–visible absorption spectroscopy. The configuration of the double-helix structure of DNA due to interaction with metallodrugs can be assigned either by hypochromism or by hyperchromism [9, 14]. Thus, hypochromism is attributed to intercalated or electrostatic binding mode, while hyperchromism is assigned to the breakage of hydrogen bonds which stabilized the secondary structure of DNA [9]. Upon the increasing of  $r$  values ( $r = [\text{complex}]/[\text{DNA}]$ ,  $[\text{DNA}] = 10^{-4}$  M) of **1–3**, a hyperchromism is observed at  $\lambda_{\text{max}} = 258$  nm for all complexes (Figure S8). The hyperchromism determined for

**Table 1** Geometric parameters and  $\text{IC}_{50}$  values of the complexes against two adenocarcinoma breast cell lines MCF-7 (hormone-dependent), MDA-MB 231 (hormone-independent) and one normal human foetal lung fibroblast cells (MRC-5 cells)

Metallodrugs	Volumes	$\text{IC}_{50}$ values ( $\mu\text{M}$ )			TPI		$K_b$ ( $\times 10^4$ ) ( $\text{M}^{-1}$ )	References
		MCF-7	MDA-MB-231	MRC-5	MCF-7	MDA-MB-231		
<b>1</b>	1131.6	$11.1 \pm 0.4$	$7.3 \pm 0.3$	$9.9 \pm 0.5$	0.9	1.4	$14.4 \pm 1.1$	*
<b>2</b>	1564.8	$9.2 \pm 0.5$	$6.4 \pm 0.2$	$5.1 \pm 0.1$	0.6	0.8	$14.2 \pm 1.7$	*
<b>3</b>	1588.9	$18.4 \pm 1.4$	$11.2 \pm 1.1$	$8.1 \pm 0.2$	0.4	0.7	$12.0 \pm 3.9$	[23]
$[\text{CuCl}(\mu_2\text{-S})\text{-tzdtH}(\text{tpSb})_2]$	1074.4	$22.6 \pm 0.6$	$29.8 \pm 0.9$	$17.4 \pm 0.7$	0.8	0.6		[23]
$[\text{CuBr}(\mu_2\text{-S})\text{-tzdtH}(\text{tpSb})_2]$	1093.7	$24.2 \pm 0.5$	$24.9 \pm 1.0$	$19.3 \pm 0.6$	0.8	0.8		[23]
$[\text{CuI}(\mu_2\text{-S})\text{-tzdtH}(\text{tpSb})_2]$	1107.3	$21.5 \pm 0.7$	$26.1 \pm 1.8$	$5.9 \pm 0.3$	0.3	0.2		[23]
Cisplatin	–	$5.5 \pm 0.4$	$26.7 \pm 1.1$	$1.1 \pm 0.2$	0.2	0.04		[23]

\*This work

tzdtH, 2-mercapto-thiazolidine

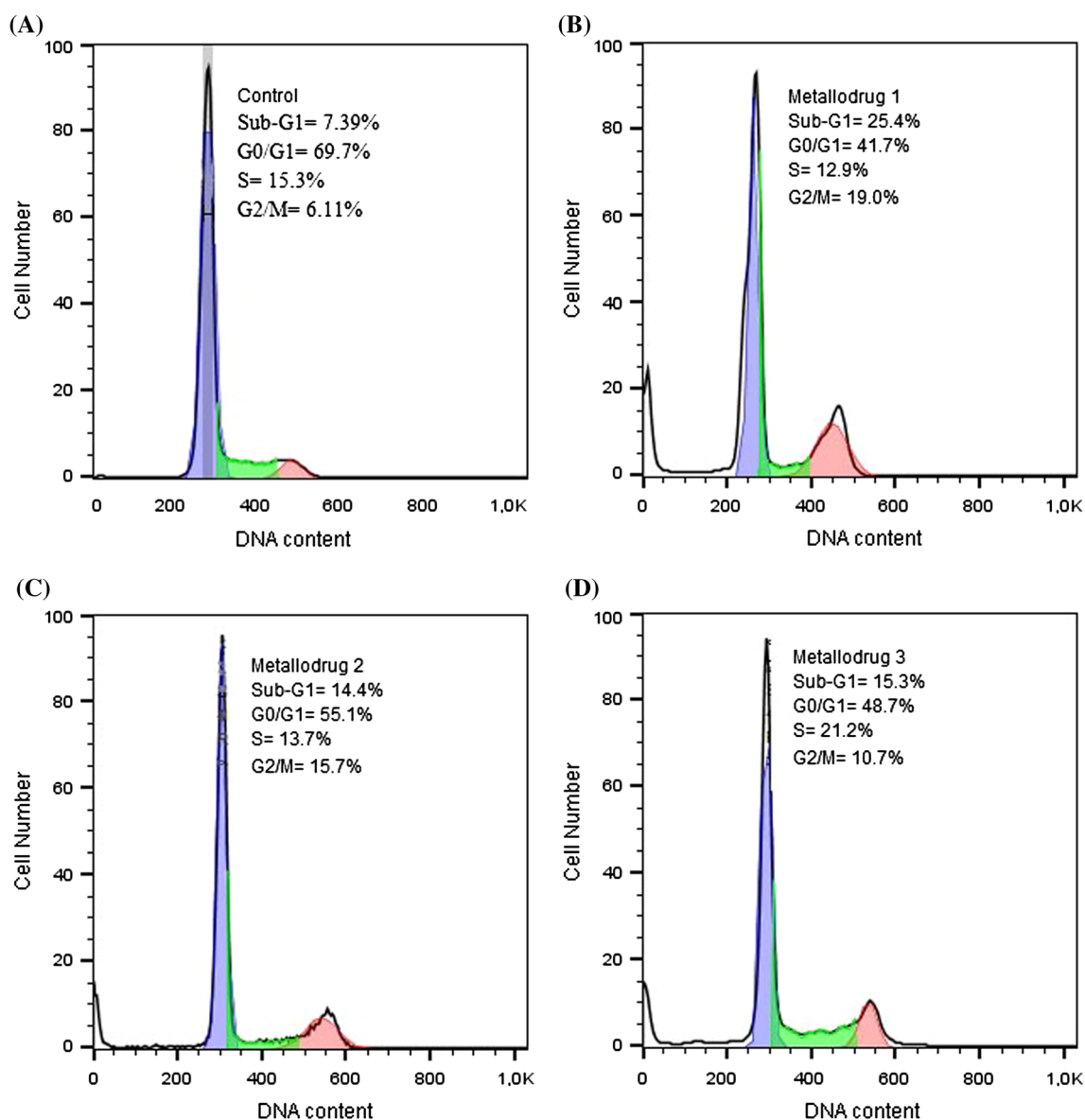


**Fig. 3** Effects on cell cycle arrest against MCF-7 cells; Untreated cells (a), **1** (b), **2** (c) and **3** (d). The relative number of cells within each cell cycle was determined by flow cytometry. Number of cells in sub-G<sub>1</sub>, G<sub>0</sub>/G<sub>1</sub>, S and G<sub>2</sub>/M phase are indicated

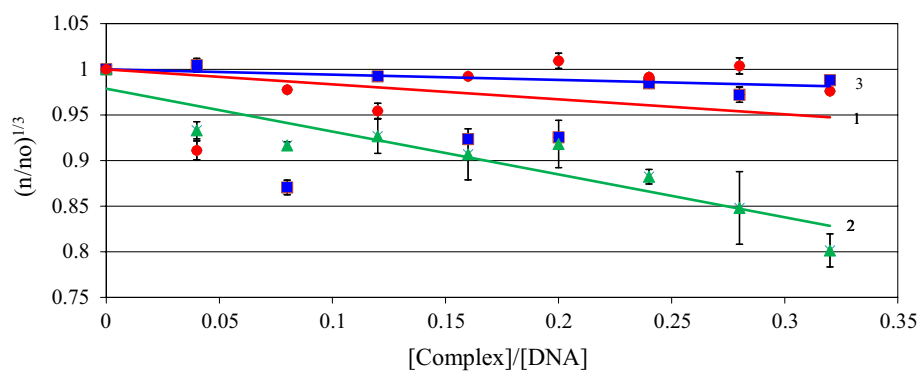
**1–3** is  $(17.1 \pm 8.8) \%$  (**1**),  $(13.7 \pm 1.6) \%$  (**2**) and  $(16.6 \pm 1.9) \%$  (**3**), respectively. Therefore, a breakage of the hydrogen bonds which stabilized the secondary structure of DNA is suggested [9].

The binding constants ( $K_b$ ) of **1–3** towards CT-DNA were determined by monitoring the absorbance changes at 300–310 nm of spectra of **1–3** (25  $\mu\text{M}$ ) with increasing concentration of CT-DNA ([CT-DNA] = 10–100  $\mu\text{M}$ ) (Figure S9). The  $K_b$  values have been obtained from Wolfe–Shimer equation [9, 10, 13–15] and they are calculated  $(14.4 \pm 1.1) \times 10^4$  (**1**),  $(14.2 \pm 1.7) \times 10^4$  (**2**) and  $(12.0 \pm 3.9) \times 10^4 \text{ M}^{-1}$  (**3**), respectively. Thus, the strength order of the binding affinity of **1–3** towards DNA is:

**1** > **2** > **3**. The corresponding  $K_b$  values for silver(I) complexes with tri-aryl-pnictogens ( $\text{Ar}_3\text{E}$ , E = P, As, Sb and Ar = Ph-, p-tolyl-, m-tolyl, o-tolyl) of the general formula  $[\text{Ag}(\text{D})(\text{Ar}_3\text{E})_n]$  (D = salicylic acid, aspirin, diclofenac, naproxen, nimesulide, etc) lie from  $5.3 \times 10^4$  to  $68.2 \times 10^4 \text{ M}^{-1}$  for tri-aryl phosphines from  $4.0 \times 10^4$  to  $25.0 \times 10^4 \text{ M}^{-1}$  for triphenylarsine and  $8.9 \pm 2.0 \times 10^4 \text{ M}^{-1}$  for triphenylantimony complex [32]. Therefore, the binding affinity of **1–3** towards DNA is within the range of those already found for silver(I) compounds.

(b) *Viscosity measurements* DNA length changes upon its incubation with an anticancer agent, and the viscosity of its solution is strongly affected. Thus, (i) if an agent intercalates

**Fig. 4** Effect of increasing concentrations of **1–3** on the relative viscosity of CT-DNA ([DNA] = 10 mM,  $r = [\text{compound}]/[\text{DNA}]$ ,  $n$  is the viscosity of DNA in the presence of **1–3** and  $n_0$  is the viscosity of DNA alone)



with the DNA strands, this results in DNA lengthening and the viscosity increase; (ii) if an agent interacts electrostatically with the DNA, no effect on DNA length is caused, and therefore, no significant change in viscosity is observed; (iii) in case that DNA strands are cleavage by an agent, the length of the DNA decreases and the viscosity decreases also significantly; and (iv) bending of the DNA helix caused by the agent reduces the viscosity [11]. Therefore, viscosity exhibits high sensitivity to the changes on DNA and it is

used for the study of the binding modes of an agent towards DNA [11]. The relative DNA solutions viscosity ( $\eta/\eta_0$ ) is correlated with the DNA length ( $L/L_0$ ) by Eq. 1 [11, 33, 34]:

$$L/L_0 = (\eta/\eta_0)^{1/3} \quad (1)$$

The solution of CT-DNA (10 mM) is incubated with an increasing amounts of **1–3** that the [compound]/[DNA] molar ratio reaches the  $r = 0.32$ . Figure 4 shows the relative specific viscosity ( $\eta/\eta_0$ )<sup>1/3</sup> versus binding ratio. The trend of lowering in the viscosity of DNA, upon increasing

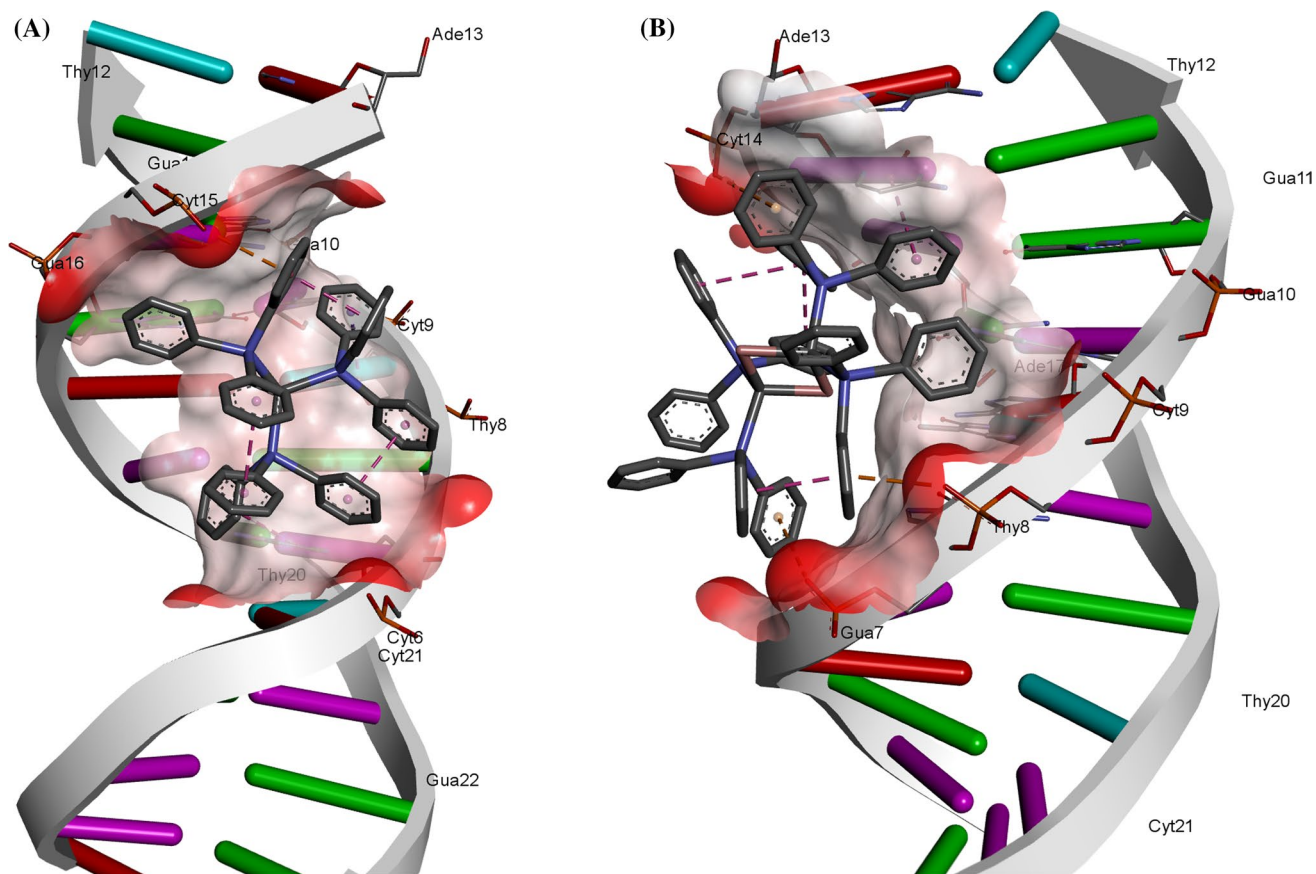


**Fig. 5** Docking poses of **1** (a) and **2** (b) at major groove of B-DNA. The corresponding CG region is marked as charged surface

concentrations of **1–3**, suggests either cleavage of the DNA strands or bending of the DNA helix [11]. This is in accordance with the breakage of hydrogen bonds that stabilize the secondary structure of DNA, which is concluded by UV measurements (see above).

**Docking studies** Docking studies attempted to depict the interactions between the synthesized metal complexes and DNA as the type of binding and interaction plays a major role in drug design and action [35]. Figure 5 shows the lowest energy binding site of complexes **1** and **2** with the DNA sequence d(ACCGACGTCGGT)<sub>2</sub>. Complexes **2** and **3** adopt similar configuration due to their similar structure. All complexes were loosely stabilized at the major groove so that the abundant phenyl rings make favourable  $\pi$ - $\pi$  and T-shaped electrostatic interactions with C9, C14, C15, G7 and G16. The lowest binding energy was calculated to -6, -5.8 and -5.6 kcal/mol for complexes **1**, **2** and **3**, respectively. Therefore, the affinity of the binding interaction between **1–3** and DNA is:  $1 > 2 > 3$  which follows the corresponding one which is determined from  $K_b$ . (The binding affinity of **1–3** towards DNA order is:  $1 > 2 > 3$ ; see above.) An important aspect of binding is van der Waals interactions and hydrophobic contacts. Although electronegative AT bases sequence are narrower and offer better van der Waals interaction space compared to GC bases, here we found that the bulk dimensions of the complexes favour GC binding. Santini et al. [36] have shown that copper–DNA binding is dependent on copper complex size, electron affinity and geometry of the formed adduct, inducing an irreversible modification of the DNA conformational structure. This rationalize the differentiation observed of **1–3** binding site towards DNA with respect to the corresponding derived by energy criterion.

Thus, compounds **1–3** initially bind in DNA with consequent cleavage of the hydrogen bonds, which are stabilizing its secondary structure [14]. This leads to the decrease of DNA length, resulting in lowering of its viscosity value [14].

## Conclusions

The known small bioactive molecules of formula [Cu(tpSb)<sub>3</sub>Cl] (**1**), [Cu<sub>2</sub>(tpSb)<sub>4</sub>Br<sub>2</sub>] (**2**) and [Cu<sub>2</sub>(tpSb)<sub>4</sub>I<sub>2</sub>] (**3**) were tested against MCF-7 (hormone-dependent (HD)) cells and MDA-MB-231 (hormone-independent (HI)) cells. A selectivity of **1–3** towards the hormone-independent MBA-MB 231 cancer cells than the hormone-dependent MCF-7 ones is observed. Compounds **1–3** are more active than cisplatin against MDA-MB 231 cells. It is noteworthy to mention here that MBA-MB 231 is triple negative breast cancer cells (TNBC). TNBC are very aggressive cancers that lack ER, PR and HER2 receptors and they do not respond to targeted treatment agents. Chemotherapy options for

women with TNBC are only managed with standard chemotherapy, such as platinum-based compounds [37]. Therefore, **1–3** might be candidates for the development new targeted chemotherapeutics against TNBC. However, upon substitution of a tpSb ligand from the coordination sphere of the homoleptic Cu(I)-Sb(II), **1–3** complexes by a tzdtH one weaken the biological activity of the compounds. The *in vitro* genotoxicity assay shows that the MN frequency of **1–3** is less than cisplatin, suggesting that the compounds can cause less genetic damage. Moreover, the metallodrugs reduce growth of MCF-7 cells through apoptosis. This is due to their DNA binding affinity. UV, viscosity measurement and computational data suggest breakage of DNA hydrogen bonds. Although electronegative AT bases sequence are narrower and offer better van der Waals interaction space compared to GC bases, the bulk dimensions of the complexes favour GC binding (Table 1) [14].

## Experimental

**Materials and instruments** All solvents used were of reagent grade; triphenyl antimony (Sigma-Aldrich, Merck) was used without further purification. Dulbecco's modified Eagle's medium (DMEM), foetal bovine serum, glutamine and trypsin were purchased from Gibco, Glasgow, UK. Phosphate buffer saline (PBS) and CT-DNA and propidium iodide were purchased from Sigma-Aldrich. Dimethyl sulfoxide and boric acid were purchased from Riedel-de Haen. Melting points were measured in open tubes with a Stuart Scientific apparatus and are uncorrected. IR spectra in the region of 4000–370 cm<sup>-1</sup> were obtained from KBr discs, with a PerkinElmer Spectrum GX FT-IR spectrophotometer. The <sup>1</sup>H NMR spectra were recorded on a Bruker AC 400 MHz FT-NMR instrument in DMSO-d<sub>6</sub> solution. A UV-1600 PC series spectrophotometer of VWR was used to obtain electronic absorption spectra. FACSCalibur flow cytometer (Becton Dickinson, San Jose, CA, USA) was obtained for the cell cycle. MDA-MB-231, MCF-7 and MRC-5 cells were purchased from the American Type Culture Collection (ATCC, Rockville, MD, USA) and the Imperial Cancer Research Fund (ICRF), London.

**Synthesis and crystallization of 1–3 complexes** **1–3** were synthesized by reacting 1.5 mmol Ph<sub>3</sub>Sb (0.352 g) with 0.5 mmol of CuCl (0.049 g) (**1**) or 0.75 mmol of CuBr (0.071 g) (**2**) and CuI (0.095 g) (**3**), in 20 mL of methanol/ acetonitrile solution under reflux for 3 h. A clear solution was finally formed. The solution was filtered off, and the clear solution was kept in the darkness at room temperature. Pale yellow crystals of **1–3** suitable for X-ray analysis were grown from the filtrate after few days.

**1**: Melting point: 145–150°C; Elemental analysis found: C: 56.30; H: 4.01%; calculated for C<sub>54</sub>H<sub>45</sub>ClCuSb<sub>3</sub>: C:

56.00; H: 3.91%. IR ( $\text{cm}^{-1}$ ) (KBr): 3043 m, 1576 m, 1477 s, 1428 vs, 1304 m, 1182 m, 1156 m, 1065 vs, 1019 s, 998 s, 916 m, 852 m, 725 vs, 691 vs, 446 vs;  $^1\text{H-NMR}$  (ppm) in DMSO- $d_6$ : 7.42–7.37 ppm (m, tpSb).

**2:** Melting point: 181–183 °C; Elemental analysis found: C: 51.05; H: 3.41%; calculated for  $\text{C}_{72}\text{H}_{60}\text{Br}_2\text{Cu}_2\text{Sb}_4$ : C: 50.90; H: 3.56%. IR ( $\text{cm}^{-1}$ ) (KBr): 3043 m, 1576 m, 1478 s, 1429 vs, 1303 m, 1180 m, 1156 m, 1067 vs, 1019 s, 995 s, 911 m, 852 m, 726 vs, 690 vs, 450 vs;  $^1\text{H-NMR}$  (ppm) in DMSO- $d_6$ : 7.41–7.38 ppm (m, tpSb).

**3:** Melting point: 171–174 °C; Elemental analysis found: C: 48.50; H: 3.22%; calculated for  $\text{C}_{72}\text{H}_{60}\text{Cu}_2\text{I}_2\text{Sb}_4$ : C: 48.23; H: 3.37%. IR ( $\text{cm}^{-1}$ ) (KBr): 3045 m, 1570 m, 1477 s, 1429 vs, 1301 m, 1182 m, 1156 m, 1065 vs, 1021 s, 995 s, 911 m, 850 m, 726 vs, 691 vs, 446 vs;  $^1\text{H-NMR}$  (ppm) in DMSO- $d_6$ : 7.40–7.36 ppm (m, tpSb).

**X-ray structure determination** Single-crystal X-ray diffraction data for **1–3** were collected on an Oxford Diffraction Supernova diffractometer, equipped with a CCD area detector utilizing Cu  $K\alpha$  ( $\lambda = 1.5418 \text{ \AA}$ ) radiation. A suitable crystal was mounted on a Hampton cryoloop with Paratone-N oil and transferred to a goniostat where it was cooled for data collection. Empirical absorption corrections (multiscan based on symmetry-related measurements) were applied using CrysAlis RED software [38]. The structures were solved by direct methods using SIR2004 [39] and refined on  $F^2$  using full-matrix least squares with SHELXL-2014/7 [40]. Software packages used were as follows: CrysAlis CCD for data collection [38], CrysAlis RED for cell refinement and data reduction [38] and WINGX for geometric calculations [41]. The non-H atoms were treated anisotropically, whereas the aromatic H atoms were placed in calculated, ideal positions and refined as riding on their respective carbon atoms.

**1:**  $\text{C}_{54}\text{H}_{45}\text{ClCuSb}_3$ , MW = 1158.14, monoclinic, space group P-1,  $a = 14.1646(5)$ ,  $b = 15.5253(5)$ ,  $c = 21.8157(8)$  Å,  $\alpha = 77.178(3)$ ,  $\beta = 84.177(3)$ ,  $\gamma = 81.118(3)^\circ$ ,  $V = 4610.5(3) \text{ \AA}^3$ ,  $Z = 4$ ,  $T = 101 \text{ K}$ ,  $\rho(\text{calc}) = 1.669 \text{ g cm}^{-3}$ ,  $\mu = 15.104 \text{ mm}^{-1}$ ,  $F(000) = 2272$ . 30933 reflections measured, 16414 unique ( $R_{\text{int}} = 0.038$ ), 13045 with  $I > 2\sigma(I)$ . The final  $R1 = 0.0368$  (for 13045 reflections with  $I > 2\sigma(I)$ ) and  $wR_2(F^2) = 0.0961$  (all data),  $S = 0.97$ .

**2:**  $\text{C}_{72}\text{H}_{60}\text{Br}_2\text{Cu}_2\text{Sb}_4$ , MW = 1699.10, monoclinic, space group P21/c,  $a = 24.1564(8)$ ,  $b = 14.0156(4)$ ,  $c = 19.8556(7)$  Å,  $\alpha = 90$ ,  $\beta = 110.116(4)$ ,  $\gamma = 90^\circ$ ,  $V = 6312.4(4) \text{ \AA}^3$ ,  $Z = 4$ ,  $T = 106 \text{ K}$ ,  $\rho(\text{calc}) = 1.788 \text{ g cm}^{-3}$ ,  $\mu = 3.657 \text{ mm}^{-1}$ ,  $F(000) = 3296$ . 32598 reflections measured, 14044 unique ( $R_{\text{int}} = 0.036$ ), 12250 with  $I > 2\sigma(I)$ . The final  $R1 = 0.0360$  (for 12250 reflections with  $I > 2\sigma(I)$ ) and  $wR_2(F^2) = 0.0801$  (all data),  $S = 1.08$ .

**3:**  $\text{C}_{72}\text{H}_{60}\text{Cu}_2\text{I}_2\text{Sb}_4$ , MW = 1793.08, monoclinic, space group P21/c,  $a = 24.4375(4)$ ,  $b = 13.9106(2)$ ,  $c = 20.2194(3)$  Å,  $\alpha = 90$ ,  $\beta = 111.169(2)$ ,  $\gamma = 90^\circ$ ,  $V = 6409.57(19) \text{ \AA}^3$ ,

$Z = 4$ ,  $T = 105 \text{ K}$ ,  $\rho(\text{calc}) = 1.858 \text{ g cm}^{-3}$ ,  $\mu = 21.771 \text{ mm}^{-1}$ ,  $F(000) = 3440$ . 23921 reflections measured, 11426 unique ( $R_{\text{int}} = 0.038$ ), 9600 with  $I > 2\sigma(I)$ . The final  $R1 = 0.0335$  (for 9600 reflections with  $I > 2\sigma(I)$ ) and  $wR_2(F^2) = 0.0819$  (all data),  $S = 0.99$ .

Supplementary data are available from CCDC, 12 Union Road, Cambridge CB2 1EZ, UK (e-mail: mailto:deposit@ccdc.cam.ac.uk), on request, quoting the deposition numbers CCDC-1917278 (**1**), CCDC-1917279 (**2**) and CCDC-1917280 (**3**).

## Biological tests

Solvents used: Stock solutions of **1–3** (0.01 M) in DMSO were freshly prepared and diluted with cell culture medium to the desired concentration. The biological experiments including the SRB assay, cell cycle and micronucleus assay were carried out in DMSO/DMEM solutions 0.005–0.3% v/v DMSO in DMEM for **1–3**. For DNA binding studies, the experiments were carried out in DMSO/buffer solutions (0.00025–0.005% v/v DMSO).

*SRB assay, Micronucleus, Cell cycle and DNA binding studies* were performed in accordance with the previous reported methods [9, 11, 14, 42].

*Computational methods* Calculations were carried out with the Gaussian03 W program package [43] at RHF/3-21G\* level of theory, based on the molecular geometry acquired via X-ray diffraction methods. All structures were fully optimized without constraints but to the bond lengths of the central 4-membered rings of complexes **2** and **3**. Similarly, magnetic shielding tensors for ghost atoms placed at different positions along the C2 axis of the  $\text{Cu}_2\text{X}_2$  (X: halogen) cluster were computed using the gauge-independent atomic orbital (GIAO) method.

For the DNA docking studies, we used the sequence 5'-D(\*AP\*CP\*GP\*GP\*AP\*CP\*GP\*TP\*CP\*GP\*GP\*T)-3' based on the 423D structure of non-complexed B-DNA found in the PDB database [44]. Molecular docking simulations were performed with Autodock Vina [45] using the default parameters. The search space covered the whole structure of the receptor and exhaustiveness was set to 12.

**Acknowledgements** This work was carried out for the fulfilment of the requirements for the B.Sc. thesis of Mr. K.K. according to the curriculum of the Department of Biological Applications and Technology of the University of Ioannina under the supervision of SKH. CNB and SKH would like to thank the Unit of Bioactivity Testing of Xenobiotics of the University of Ioannina for providing access to the facilities. CNB and SKH would like to thank the Atherothrombosis Research Centre of the University of Ioannina for providing access to the flow cytometer and to the fluorescence microscopy. This research has been co-financed by the European Union and Greek national funds through the Operational Program Competitiveness, Entrepreneurship and Innovation, under the call RESEARCH – CREATE – INNOVATE (Project Code: T1EDK-02990).

## Compliance with ethical standards

**Conflict of interest** The authors declare that they have no conflict of interest.

## References

- Harbeck N, Penault-Flloca F, Cortes J, Gnant M, Houssami N, Poortmans P, Ruddy K, Tsang J, Cardoso F (2019) Breast cancer. *Nat Rev Dis Primers* 5, Article citation ID: 66. <https://doi.org/10.1038/s41572-019-0111-2>
- Shpakovsky DB, Banti CN, Beaulieu-Houle G, Kourkoumelis N, Manoli M, Manos MJ, Tasiopoulos AJ, Hadjidakou SK, Milaeva ER, Charalabopoulos K, Bakas T, Butler IS, Hadjiladis N (2012) Synthesis, structural characterization and in vitro inhibitory studies against human breast cancer of the bis-(2,6-di-tert-butylphenol)tin(IV) dichloride and its complexes. *Dalton Trans* 41:14568. <https://doi.org/10.1039/C2DT31527K>
- Mazumdar A, Tahaney WM, Reddy Bollu L, Poage G, Hill J, Zhang Y, Mills GB, Brown PH (2019) The phosphatase PPM1A inhibits triple negative breast cancer growth by blocking cell cycle progression. *npj Breast Cancer* 5, Article number: 22. <https://doi.org/10.1038/s41523-019-0118-6>
- Theodossiou TA, Ali M, Grigalavicius M, Grallert B, Dillard P, Oliver Schink K, Olsen CE, Wälchli S, Inderberg EM, Kubin A, Peng Q, Berg K (2019) Simultaneous defeat of MCF7 and MDA-MB-231 resistances by a hypericin PDT-tamoxifen hybrid therapy. *npj Breast Cancer* 5, Article number: 13. <https://doi.org/10.1038/s41523-019-0108-8>
- Hero T, Bühler H, Kouam PN, Priesch-Grzeszowiak B, Lateit T, Adamietz IA (2019) The triple-negative breast cancer cell line MDA-MB 231 is specifically inhibited by the ionophore salinomycin. *Anticancer Res* 39:2821–2827. <https://doi.org/10.21873/anticancer.13410>
- Ahmad Khan R., Usman M, Dhivya R, Balaji P, Alsalmeh A, AlLohedan H, Arjmand F, AlFarhan K, Abdulkader Akbarsha M, Marchetti F, Pettinari C, Tabassum S (2017) Heteroleptic copper(I) complexes of “scorpionate” bis-pyrazolyl carboxylate ligand with auxiliary phosphine as potential anticancer agents: an insight into cytotoxic mode. *Sci Rep* 7, Article number: 45229. <https://doi.org/10.1038/srep45229>
- Komarnicka UK, Starosta R, Płotek M, de Almeida RFM, Jeżowska-Bojczuk M, Kyzioł A (2016) Copper(I) complexes with phosphine derived from sparfloxacin. Part II: a first insight into the cytotoxic action mode. *Dalton Trans* 45:5052–5063. <https://doi.org/10.1039/C5DT04011F>
- Hadjidakou SK, Ozturk II, Banti CN, Kourkoumelis N, Hadjiladis N (2015) Recent advances on antimony(III/V) compounds with potential activity against tumor cells. *J Inorg Biochem* 153:293–305. <https://doi.org/10.1016/j.jinorgbio.2015.06.006>
- Banti CN, Papatriantafyllopoulou C, Manoli M, Tasiopoulos AJ, Hadjidakou SK (2016) Nimesulide silver metallodrugs, containing the mitochondriotropic, triaryl derivatives of pnicogen; Anticancer activity against human breast cancer cells. *Inorg Chem* 55:8681–8696. <https://doi.org/10.1021/acs.inorgchem.6b01241>
- Chrysouli MP, Banti CN, Kourkoumelis N, Panayiotou N, Tasiopoulos AJ, Hadjidakou SK (2018) Chloro(triphenylphosphine) gold(I) a forefront reagent in gold chemistry as apoptotic agent for cancer cells. *J Inorg Biochem* 179:107–120. <https://doi.org/10.1016/j.jinorgbio.2017.11.004>
- Latsis GK, Banti CN, Kourkoumelis N, Papatriantafyllopoulou C, Panagiotou N, Tasiopoulos A, Douvalis A, Kalamounias AG, Bakas T, Hadjidakou SK (2018) Poly organotin acetates against DNA with possible implementation on human breast cancer. *Int J Mol Sci* 19:2055–2072. <https://doi.org/10.3390/ijms19072055>
- Gkaniatsou EI, Banti CN, Kourkoumelis N, Skoulika S, Manoli M, Tasiopoulos AJ, Hadjidakou SK (2015) Novel mixed metal Ag(I)-Sb(III)-metallotherapeutics of the NSAIDs, aspirin and salicylic acid: enhancement of their solubility and bioactivity by using the surfactant CTAB. *J Inorg Biochem* 150:108–119. <https://doi.org/10.1016/j.jinorgbio.2015.04.014>
- Polychronis NM, Banti CN, Raptopoulou CP, Psycharis V, Kourkoumelis N, Hadjidakou SK (2019) Non steroidal anti-inflammatory drug (NSAIDs) in breast cancer chemotherapy; antimony(V) salicylate a DNA binder. *Inorg Chim Acta* 489:39–47. <https://doi.org/10.1016/j.ica.2019.02.004>
- Banti CN, Giannoulis AD, Kourkoumelis N, Owczarzak AM, Poyraz M, Kubicki M, Charalabopoulos K, Hadjidakou SK (2012) Mixed ligand–silver(I) complexes with anti-inflammatory agents which can bind to lipoxygenase and calf-thymus DNA, modulating their function and inducing apoptosis. *Metallomics* 4:545–560. <https://doi.org/10.1039/c2mt20039b>
- Banti CN, Giannoulis AD, Kourkoumelis N, Owczarzak A, Kubicki M, Hadjidakou SK (2014) Novel metallo-therapeutics of the NSAID naproxen. Interaction with intracellular components that leads the cells to apoptosis. *Dalton Trans* 43:6848–6863. <https://doi.org/10.1039/c3dt53175a>
- Poyraz M, Banti CN, Kourkoumelis N, Dokorou V, Manos MJ, Simčič M, Golič-Grdadolnik S, Mavromoustakos T, Giannoulis AD, Verginadis II, Charalabopoulos K, Hadjidakou SK (2011) Synthesis, structural characterization and biological studies of novel mixed ligand Ag(I) complexes with triphenylphosphine and aspirin or salicylic acid. *Inorg Chim Acta* 375:114–121. <https://doi.org/10.1016/j.ica.2011.04.032>
- Batsala GK, Dokorou V, Kourkoumelis N, Manos MJ, Tasiopoulos AJ, Mavromoustakos T, Simčič M, Golič-Grdadolnik S, Hadjidakou SK (2012) Copper(I)/(II) or silver(I) salts towards 2-mercaptopyrimidine; An exploration of a chemical variability with possible biological implications. *Inorg Chim Acta* 382:146–157. <https://doi.org/10.1016/j.ica.2011.10.024>
- Bowmaker GA, Hart RD, De Silva EN, Skelton BW, White AH (1997) Lewis-base adducts of Group 11 Metal(I) compounds. LXX synthesis, spectroscopy and structural systematics of 1:2 binuclear adducts of copper(I) halides with triphenylstibine, [(Ph<sub>3</sub>Sb)<sub>2</sub>Cu(-X)<sub>2</sub>Cu(SbPh<sub>3</sub>)<sub>2</sub>], X = Cl, Br, I. *Aust J Chem* 50:621–626. <https://doi.org/10.1071/C96036>
- Zhang Q-F, Zeng D-X, Xin X-Q, Wong W-T (1999) Solid state synthesis and structural characterization of binuclear Cu(I)-SbPh<sub>3</sub>-3 Complex [Cu(SbPh<sub>3</sub>)<sub>2</sub>]<sub>2</sub>. *Jiegou Huaxue (Chin J Struct Chem)* 18:356
- Paizanos K, Charalampou D, Kourkoumelis N, Kalpogiannaki D, Hadjiarapoglou L, Spanopoulou A, Lazarou K, Manos MJ, Tasiopoulos AJ, Kubicki M, Hadjidakou SK (2012) Synthesis and structural characterization of new Cu(I) complexes with the antithyroid drug 6-n-propyl-thiouracil. Study of the Cu(I)-catalyzed intermolecular cycloaddition of iodonium ylides towards benzo[b]furans with pharmaceutical implementations. *Inorg Chem* 51:12248–12259. <https://doi.org/10.1021/ic3014255>
- Rheingold AL, Fountain ME (1984) Crystal and molecular structure of [(C<sub>6</sub>H<sub>5</sub>)<sub>3</sub>Sb]<sub>3</sub>CuCl-CHCl<sub>3</sub>. *J Crystallogr Spectrosc Res* 14:549. <https://doi.org/10.1007/BF01182141>
- Reichle WT (1971) Preparation, physical properties and reactions of copper(I)-triphenyl-m complexes (M = P, As, Sb). *Inorg Chim Acta* 5:325–332. [https://doi.org/10.1016/S0020-1693\(00\)95939-5](https://doi.org/10.1016/S0020-1693(00)95939-5)
- Tsiatouras V, Banti CN, Grzeskiewicz AM, Rossos G, Kourkoumelis N, Kubicki M, Hadjidakou SK (2016) Structural, photolysis and biological studies of novel mixed metal Cu(I)-Sb(III)

- mixed ligand complexes. *J Photochem Photobiol B* 163:261–268. <https://doi.org/10.1016/j.jphotobiol.2016.08.041>
24. PvR Schleyer, Maerker C, Dransfeld A, Jiao H, Hommes NJRvE (1996) Nucleus-independent chemical shifts: a simple and efficient aromaticity probe. *J Am Chem Soc* 118:6317–6318. <https://doi.org/10.1021/ja960582d>
25. Huang X, Zhai HJ, Kiran B, Wang LS (2005) Observation of d-orbital aromaticity. *Angew Chem* 44:7251–7254. <https://doi.org/10.1002/anie.200502678>
26. Kajstura M, Dorota Halicka H, Pryjma J, Darzynkiewicz Z (2007) Discontinuous fragmentation of nuclear DNA during apoptosis revealed by discrete “sub-G1” peaks on DNA content histograms. *Cytom A* 71A:125–131. <https://doi.org/10.1002/cyto.a.20357>
27. Gou Y, Qi J, Ajayi J-P, Zhang Y, Zhou Z, Wu X, Yang F, Liang H (2015) Developing anticancer copper(II) pro-drugs based on the nature of cancer cells and the human serum albumin carrier IIA subdomain. *Mol Pharm* 12:3597–3609. <https://doi.org/10.1021/acs.molpharmaceut.5b00314>
28. Lee S-H, Kim D-K, Seo Y-R, Woo K-M, Kim C-S, Cho M-H (1998) Nickel(II)-induced apoptosis and G2/M enrichment. *Exp Mol Med* 30:171–176. <https://doi.org/10.1038/emm.1998.25>
29. Kohn EA, Ruth ND, Kay Brown M, Livingstone M, Eastman A (2002) Abrogation of the S phase DNA damage checkpoint results in S phase progression or premature mitosis depending on the concentration of 7 hydroxystaurosporine and the kinetics of Cdc25C activation. *J Biol Chem* 277:26553–26564. <https://doi.org/10.1074/jbc.M202040200>
30. Galindo-Murillo R, Carlos Garcia-Ramos J, Ruiz-Azuara L, Cheatham TE, Cortes-Guzman F (2015) Intercalation processes of copper complexes in DNA. *Nucl Acids Res* 43:5364–5376. <https://doi.org/10.1093/nar/gkv467>
31. Serment-Guerrero J, Elena Bravo-Gomez M, Lara-Rivera E, Ruiz-Azuara L (2017) Genotoxic assessment of the copper chelated compounds Casiopeinas: clues about their mechanisms of action. *J Inorg Biochem* 166:68–75. <https://doi.org/10.1016/j.jinorgbio.2016.11.007>
32. Banti CN, Papatrifiantafyllopoulou C, Tasiopoulos AJ, Hadjikakou SK (2018) New metallo-therapeutics of NSAIDs against human breast cancer cells. *Eur J Med Chem* 143:1687–1701. <https://doi.org/10.1016/j.ejmech.2017.10.067>
33. Kellett A, Molphy Z, Slator C, McKee V, Farrell NP (2019) Molecular methods for assessment of non-covalent metallodrug–DNA interactions. *Chem Soc Rev* 48:971–988. <https://doi.org/10.1039/C8CS00157J>
34. Li D-D, Tian J-L, Gu W, Liu X, Yan S-P (2010) A novel 1,2,4-triazole-based copper(II) complex: synthesis, characterization, magnetic property and nuclease activity. *J Inorg Biochem* 104:171–179. <https://doi.org/10.1016/j.jinorgbio.2009.10.020>
35. Boer DR, Canals A, Coll M (2009) DNA-binding drugs caught in action: the latest 3D pictures of drug-DNA complexes. *Dalton Trans.* <https://doi.org/10.1039/b809873p>
36. Santini C, Pellei M, Gandin V, Porchia M, Tisato F, Marzano C (2014) Advances in copper complexes as anticancer agents. *Chem Rev* 114:815–862. <https://doi.org/10.1021/cr400135x>
37. Wawruszak A, Luszczki JJ, Kalafut J, Okla K, Halasa M, Rivero-Muller A, Stepulak A (2019) Additive pharmacological interaction between cisplatin (CDDP) and histone deacetylase inhibitors (HDIs) in MDA-MB-231 triple negative breast cancer (TNBC) cells with altered Notch1 activity—an isobolographic analysis. *Int J Mol Sci* 20:3663–3679. <https://doi.org/10.3390/ijms20153663>
38. Diffraction Oxford (2008) CrysAlis CCD and CrysAlis RED. Oxford Diffraction Ltd., Abingdon
39. Burla MC, Caliandro R, Camalli M, Carrozzini B, Cascarano GL, De Caro L, Giacovazzo C, Polidori G, Spagna R (2005) SIR2004: an improved tool for crystal structure determination and refinement. *J Appl Cryst* 38:381–388. <https://doi.org/10.1107/S002188980403225X>
40. Sheldrick GM (2014) SHELXL-2014/7, program for refinement of crystal structures. University of Göttingen, Göttingen
41. Farrugia LJ (1999) WinGX suite for small-molecule single-crystal crystallography. *J Appl Cryst* 32:837–838. <https://doi.org/10.1107/S0021889899006020>
42. Banti CN, Hadjikakou SK (2019) Evaluation of genotoxicity by micronucleus assay in vitro and by *Allium cepa* test in vivo. *Bio-Protocol* 9:3311. <https://doi.org/10.21769/BioProtoc.3311>
43. Frisch MJ, Trucks GW, Schlegel HB, Scuseria GE, Robb MA, Cheeseman JR, Montgomery JA Jr, Vreven T, Kudin KN, Burant JC, Millam JM, Iyengar SS, Tomasi J, Barone V, Mennucci B, Cossi M, Scalmani G, Rega N, Petersson GA, Nakatsuji H, Hada M, Ehara M, Toyota K, Fukuda R, Hasegawa J, Ishida M, Nakajima T, Honda Y, Kitao O, Nakai H, Klene M, Li X, Knox JE, Hratchian HP, Cross JB, Bakken V, Adamo C, Jaramillo J, Gomperts R, Stratmann RE, Yazyev O, Austin AJ, Cammi R, Pomelli C, Ochterski JW, Ayala PY, Morokuma K, Voth GA, Salvador P, Dannenberg JJ, Zakrzewski VG, Dapprich S, Daniels AD, Strain MC, Farkas O, Malick DK, Rabuck AD, Raghavachari K, Foresman JB, Ortiz JV, Cui Q, Baboul AG, Clifford S, Cioslowski J, Stefanov BB, Liu G, Liashenko A, Piskorz P, Komaromi I, Martin RL, Fox DJ, Keith T, Al-Laham MA, Peng CY, Nanayakkara A, Challacombe M, Gill PMW, Johnson B, Chen W, Wong MW, Gonzalez C, Pople JA (2004) Gaussian 03, Revision C.02. Gaussian, Wallingford
44. Rozenberg H, Rabinovich D, Frolov F, Hegde RS, Shakked Z (1998) Structural code for DNA recognition revealed in crystal structures of papillomavirus E2-DNA targets. *Proc Natl Acad Sci USA* 95:15194–15199. <https://doi.org/10.1073/pnas.95.26.15194>
45. Trott O, Olson AJ (2010) AutoDock Vina: Improving the speed and accuracy of docking with a new scoring function, efficient optimization, and multithreading. *J Comput Chem* 31:455–461. <https://doi.org/10.1002/jcc.21334>

**Publisher's Note** Springer Nature remains neutral with regard to jurisdictional claims in published maps and institutional affiliations.